

Impedance Spectroscopy of High-Molecular Poly(ethylene) with Carbon Nanotubes

N. A. Drokin*, A. V. Fedotova, G. A. Glushchenko, and G. N. Churilov

Kirensky Institute of Physics, Siberian Branch, Russian Academy of Sciences,
Akademgorodok 50, Krasnoyarsk, 660036 Russia

*e-mail: drokin@iph.krasn.ru

Received June 9, 2009

Abstract—The impedance spectra of composite materials based on the high-molecular poly(ethylene) modified by carbon nanotubes have been investigated. A numerical method has been proposed for reconstructing the relaxation time distribution function of the active (R) and reactive (C) elements of a sample directly from the experimentally obtained frequency dependence of the real and imaginary components of the impedance. It has been shown that, with an increase in the concentration of carbon nanotubes, the electrical conductivity of the samples under study increases and their impedance characteristics are described by a nonmonotonic relaxation time distribution function.

DOI: 10.1134/S1063783410030303

1. INTRODUCTION

Composite materials based on the poly(ethylene) modified by carbon fillers (carbon black, fullerenes, carbon nanotubes) are the subject of numerous studies in view of their application in electrical engineering and electronics [1–3]. Fillers prepared from carbon nanotubes are of special interest, because mechanically strong fibers of nanotubes increase the wear resistance of the material as a whole and the spatial network of conductive chains formed in the poly(ethylene) matrix provides a high conductivity of the composite with a relatively low content of the filler. The electrophysical properties of these conductive polymer composites can be conveniently studied by measuring the impedance $Z^* = Z' - iZ''$ of a measuring cell with a sample. Here, Z' and Z'' are the active (real) and reactive (imaginary) parts of the impedance vector, which make it possible to determine and analyze both dielectric and conductive properties of materials [4]. However, the determination of these characteristics is a difficult problem, which consists in establishing the relationship of the conduction and bias current to the physical properties of the materials under study. The main method for these studies consists in constructing a model of an electric circuit in which the active and reactive elements in their sense correspond to the simulated processes that proceed as the alternating electric current flows in the sample. The choice of one or another electric circuit is determined individually according to the behavior of $|Z|$, the phase shift φ between the current and voltage, and the impedance locus constructed in the coordinates Z' and Z'' (the Nyquist diagram) [5]. Since the response of the system under study to an alternating electric

field is caused by numerous factors, e.g., the heterogeneity of the medium and volume or near-electrode polarization, all models are limited to some extent. In the present work, we investigate the impedance of samples of ultra-high molecular weight poly(ethylene) (UHMWPE) with carbon nanotubes (CNTs) and consider some methodological problems of the analysis of the data obtained.

2. SAMPLE PREPARATION AND EXPERIMENTAL TECHNIQUE

A powder of UHMWPE with a molecular mass $M \geq 10^6$ g/mol was mixed with a carbon-containing mixture partially cleaned from nanodispersed particles (81 vol % CNTs and 19 vol % of nanodispersed carbon). The amounts of the UHMWPE powder and the above mixture were calculated so that the maximum volume content of nanotubes in the UHMWPE samples did not exceed 8%. The UHMWPE + CNT mixture was heated to the softening temperature of poly(ethylene), $T \sim 130\text{--}140^\circ\text{C}$, directly in a press-mold under a pressure of 80 bar. Disks with a diameter of 14 mm and a thickness of 0.5 mm were produced. The samples were held at a temperature $T = 100^\circ\text{C}$ for several hours for the stabilization of their properties.

In this work, a lumped measuring cell was an electric capacitor formed by two circular metal electrodes with a diameter of 14 mm, between which the sample under study was clamped. The end surface of the samples was covered with graphite in order to reduce the electrode resistance. The cell in a special holder was placed in a thermostat with the temperature controlled from 20 to 150°C and was connected by transmission

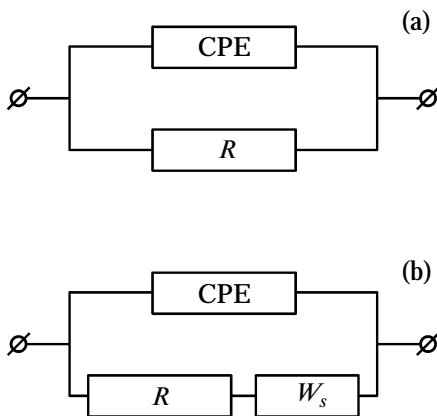


Fig. 1. Equivalent circuits.

lines to WK 4270 and BM 538 T impedance meters operating in the frequency ranges $f = 0.0001$ –1 and 1–100 MHz, respectively. The additional capacitance of the conducting transmission lines was compensated for by automatic calibration of the impedance meters with the disconnected measuring cell.

3. RESULTS AND DISCUSSION

In the experiment, we measured the magnitude of the impedance $|Z|$ and the phase shift φ between the current and voltage. Then, we calculated the real ($Z' = |Z|\cos\varphi$) and imaginary ($Z'' = |Z|\sin\varphi$) parts of the impedance. In order to construct the equivalent circuit and to calculate the resistance–capacitance properties of the composites under study, the substances used in our work should be considered strongly inhomogeneous media in which the fibers of nanotubes form complex labyrinth structures. Fibers connected to one another over the depth of the sample can be treated as an active resistor connected between the electrodes (the leakage resistor). Since the nanotubes have a high conductivity, we can assume that the main contribution to the impedance is made by the contact between the nanotubes. The regions of the sample containing isolated clusters of nanotubes form conducting inclusions chaotically distributed in the poly(ethylene) matrix. In the alternating electric field, accumulation and redistribution of charges should take place at the boundaries of these inclusions, which distorts the initial internal electric field. This process is called the Maxwell–Wagner interfacial or volume polarization [5]. At low frequencies, the surface charge has time to follow the field and the dielectric losses are small. In the high-frequency range, the dielectric losses are also small because the polarization has no time to be attained for the half-period of the field. In the intermediate frequency range, the permittivity and impedance dispersions characterized by the relaxation time $\langle\tau\rangle = RC$ manifest themselves. Here, R and C are the mean values of the resistance and capac-

itance of clusters, which in the initial approximation can be simulated by a parallel RC circuit. However, numerous studies of heterogeneous media show that highly conductive parts of the sample form statistically inhomogeneous regions with different relaxation times. In some cases, experimental values of $Z(\omega)$ can be approximated by an equivalent circuit involving multilink parallel R_kC_k circuits, whose impedance can be written in the form

$$Z(\omega) = \sum_{k=1}^m (R_k^{-1} + j\omega C_k)^{-1}, \quad (1)$$

where m is the number of links and j is an imaginary number. However, a more effective approach to the approximation of experimental impedance spectra is to use universal frequency-dependent elements simulating a wide class of electrotechnical materials and electrochemical systems. One of these elements is, e.g., the constant phase element (CPE), for which the impedance is described by the expression [6]

$$Z_{\text{CPE}} = 1/[Y_0(j\omega)^n], \quad (2)$$

where Y_0 is a frequency-dependent factor and n is the exponent determining the character of the frequency dependence of the impedance. For the integers $n = 1, 0$, and -1 , the constant phase element degenerates into elements with RCL lumped parameters. For $n < 1$, the constant phase element describes a frequency-dependent element lumped $C(\omega)$.

In the analysis of some objects, Eq. (2) can be modified to a more complicated form, e.g., to a constant phase element with a given conductivity at $\omega \rightarrow 0$ (the Warburg element W_s) [7]. Typical equivalent circuits using these elements for the approximation of experimental impedance spectra $Z(\omega)$ are shown in Fig. 1. The numerical values of the active and reactive parameters of these circuits were determined by means of the specialized EIS Spectrum Analyzer program. A specific evaluation for the quality of approximation of the experimental values $Z' = |Z|\cos\varphi$ and $Z'' = |Z|\sin\varphi$ and the calculation is a comparison between the corresponding loci. For example, Figs. 2a and 2b show the loci for the UHMWPE samples containing 4 and 6 vol % CNTs, respectively. In this case, the equivalent circuits used for the samples with 4 and 6 vol % CNTs are shown in Figs. 1a and 1b, respectively. It should be noted that, at $\omega \rightarrow 0$, the value of Z coincides with the static resistance, which is $R = 49700$ and 4700Ω for these two samples. With an increase in the frequency of the electric field to 100 MHz, the impedance of both samples decreases to ~ 50 – 80Ω and is almost equal to the reactance. It can be seen from Fig. 2 that the loci obtained from the experiment and constructed with the use of the equivalent circuits for both samples coincide and have the same form of a distorted arc of a circle with the center lying below the

abscissa axis. For the sample with 4 vol % CNT from Fig. 2a, we obtained the following parameters of the elements of the equivalent circuit: $R = 49700 \Omega$, $Z_{\text{CPE}} = 2 \times 10^{-9}$, and $n = 0.895$. Here, the coefficient n determines the displacement of the center of the semi-circle with respect to the abscissa axis. For the second samples with 6 vol % of CNTs (with a lower resistance), the locus is characterized by an asymmetry, which is taken into account by introducing the Wartburg element W_s into the equivalent circuit. We obtained the following parameters of the equivalent circuit: $R = 4900 \Omega$, $Z_{\text{CPE}} = 2 \times 10^{-9}$, $n = 0.895$, and the active and reactive Wartburg components $W_{\text{sr}} = 150000$ and $W_{\text{sc}} = 0.006$.

As can be seen, the calculated loci well approximate the experimental impedance spectra, which indicates that the samples contain clusters that differ statistically in the resistance and mutual capacitance. In this case, it is important to know the range in which the relaxation times are distributed. In the general case, the character of the relaxation time distribution should be described by introducing an analytically specified relaxation time distribution function $g(\tau)$ into the dispersion relation for the impedance [8, 9]:

$$Z^* = R_\infty + \Delta \int_0^\infty \frac{g(\ln \tau)}{1 + i\omega\tau} d(\ln \tau). \quad (3)$$

Here, $\Delta R = R_c - R_\infty$, where R_c is the resistance of the sample at the direct current and R_∞ is the resistance at ultimately high frequencies. The normalization condition is written in the form

$$\int_0^\infty g(\ln \tau) d(\ln \tau) = 1. \quad (4)$$

It should be noted that a microscopic model of complex polarization and conduction processes in strongly inhomogeneous heterogeneous media can be constructed and analytically appropriate relaxation time distribution function for the approximation of impedance spectra can be specified only in exceptional cases. Therefore, in world practice, it becomes especially important to develop numerical methods for determining the relaxation time distribution functions directly from the experimentally measured spectra of the permittivity or the impedance components [10–12]. In [13], a specialized algorithm using a regularization procedure for determining the relaxation time distribution functions has been developed for the analysis of the dispersion in the real part of the permittivity of liquid crystals. In the present work, this algorithm was modified for finding the relaxation time distribution function from the data on the dispersion of the real and imaginary parts of the impedance. In this method, the impedance spectra are represented by

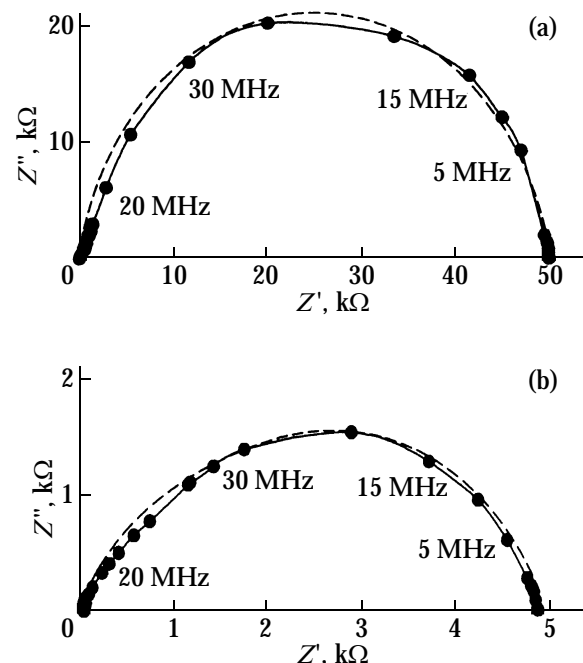


Fig. 2. Impedance loci for the UHMWPE samples with (a) 4 and (b) 6 vol % CNTs. Points and solid lines indicate the experimental data, and dashed lines represent the results of the calculations.

histograms constructed by separating the frequency range of the spectra $Z'(\omega)$ and $Z''(\omega)$ into a given number N of equal intervals. In this case, each rectangle in the histogram corresponds to a mean frequency ω_i and the corresponding relaxation time τ_i . The sought distribution function is reconstructed by minimization of the functional

$$\chi(g) = \sum_{i=1}^N \{[Z'(\omega_i) \pm \Delta Z'(\omega_i)] - Z'_{\text{calc}}(\omega_i)\}^2, \quad (5)$$

where $Z'(\omega)$ is the experimental spectrum smoothed by an appropriate approximation and $Z'_{\text{calc}}(\omega)$ is the impedance calculated by expression (3) in which the integral is replaced by the corresponding sum. As the initial relaxation time distribution function, the values of $Z''(\omega)$ are used. In Eq. (5), $\Delta Z'(\omega)$ is the regularization parameter providing the stability of the algorithm. This parameter simulates the artificial measuring error by generating small random numbers $\pm \sigma, \approx 0.05-0.15$, which are added to the smoothed spectrum $Z'(\omega)$. The relaxation time distribution functions obtained for two samples are presented in Fig. 3. It can be seen from this figure that, for the sample with 4 vol % CNTs (Fig. 3a), the relaxation time distribution function has the form of an almost symmetric Lorenz curve with the “wings” extended to the regions of short and long relaxation times. The maximum of this curve corresponds to the relaxation time $\tau \approx 6.2 \times 10^{-6}$ s, which is

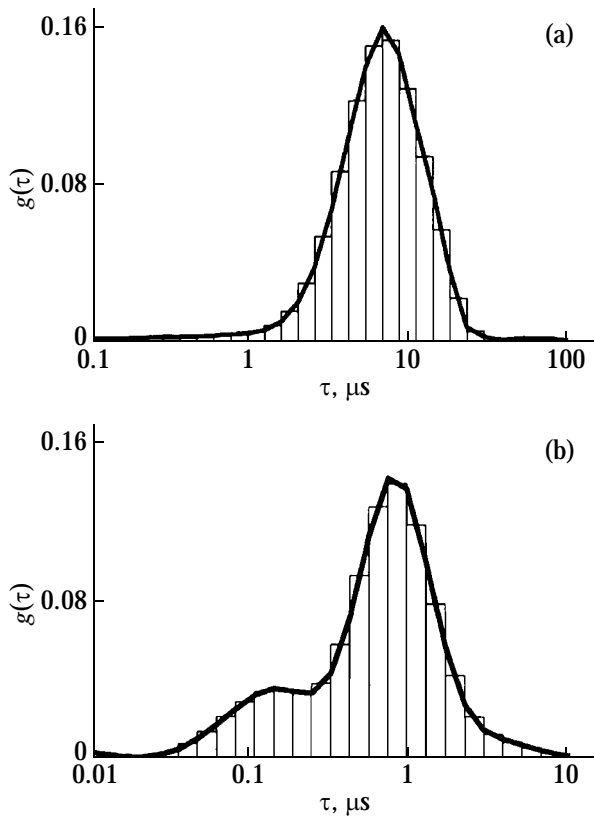


Fig. 3. Relaxation time distribution functions for the UHMWPE samples with (a) 4 and (b) 6 vol % CNTs.

close to the value $\tau = 5.86 \times 10^{-6}$ s that is observed at the frequency at which the maximum of the half-circle of the locus is situated (Fig. 3a). The broadening of the relaxation time distribution function is associated with the existence of a set of additional relaxation times in the range $3 \times 10^{-5} \leq \tau \leq 1 \times 10^{-6}$ s.

For the UHMWPE sample with 6 vol % CNTs under investigation, the relaxation time distribution function (Fig. 3b) exhibit two maxima, which correspond to the times $\tau_{lf} = 9.0 \times 10^{-7}$ and 1.4×10^{-7} s. This transformation of the relaxation time distribution function was typical of all check samples with a high through conductivity.

It is of interest to study the UHMWPE sample with 8 vol % of carbon condensate containing only 40 vol % CNTs as a function of the temperature. The results of the measurements are presented in Fig. 4. As can be seen from this figure, only one maximum in the relaxation time distribution function is observed ($\tau = 8 \times 10^{-5}$ s) at room temperature. In this case, the dc resistance of the sample is $Z(0) = 27000 \Omega$. With an increase in the temperature to 100°C , the relaxation times decrease to $\tau = 1 \times 10^{-5}$ s. At $T = 120^\circ\text{C}$, the relaxation time distribution function already has two maxima with the relaxation times $\tau_1 = 8 \times 10^{-6}$ s and

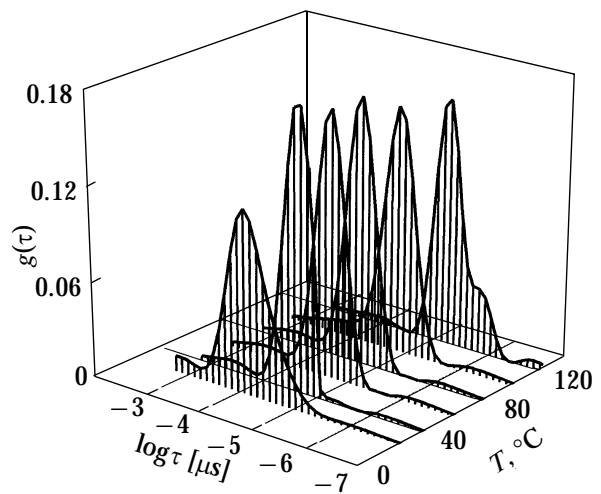


Fig. 4. Temperature dependence of the relaxation time distribution function.

$\tau_2 = 1.2 \times 10^{-6}$ s. The resistance of the sample at this temperature decreases to $Z(0) = 2200 \Omega$. These changes show that the nonmonotonic form of the relaxation time distribution function and the additional relaxation times in the range of higher frequencies can arise not only with an increase in the concentration of the impurity but with an increase in the temperature as well.

4. CONCLUSIONS

Thus, in this work, we have proposed a method that allows one to determine the typical relaxation times of the active and reactive elements of the material under study by reconstructing the relaxation time distribution function directly from the experimentally measured frequency dependences of the impedance. This makes it possible to avoid a complex and time-consuming search for an appropriate equivalent circuit simulating dielectric and conductive properties of a material. The pronounced maximum in the relaxation time distribution function for samples with a limited conductivity ($R \geq 48000 \Omega$) most likely corresponds to the averaged relaxation time of CNT–UHMWPE–CNT conductive inclusions statistically distributed over the volume of the sample. The appearance of the second relaxation time with an increase in the filler concentration or in the temperature can be caused by the existence of more complex inclusions, containing, e.g., carbon particles. One more factor responsible for the appearance of this maximum can be a specific transition layer at the interface between the matrix and the filler [14]. This question calls for additional studies of both electrical and dielectric properties of this type of composites.

ACKNOWLEDGMENTS

This study was supported by the Presidium of the Russian Academy of Sciences (project no. 27.1), the Siberian Branch of the Russian Academy of Sciences (integration project no. 5), and the Council on Grants from the President of the Russian Federation (grant no. 3818.2008.3).

REFERENCES

1. V. E. Krikorov and L. A. Kolmakova, *Conducting Polymer Materials* (Énergoatomizdat, Moscow, 1984) [in Russian].
2. V. R. Sichkar', B. A. Briskman, and I. G. Bukanov, *Vysokomol. Soedin., Ser. A* **39** (6), 1054 (1997) [*Polym. Sci., Ser. A* **39** (6), 720 (1997)].
3. M. Velikova, *Eur. Polym. J.* **37**, 1255 (2001).
4. E. Barsoukov and J. R. Macdonald, *Impedance Spectroscopy: Theory, Experiment, and Applications* (Wiley, New York, 2005).
5. A. K. Ivanov-Shits and I. V. Murin, *Solid State Ionics* (St. Petersburg State University, St. Petersburg, 2000), Vol. 1 [in Russian].
6. Z. B. Stočnov, B. M. Grafov, B. Savova-Stročnova, and V. V. Elkin, *Electrochemical Impedance* (Nauka, Moscow, 1991) [in Russian].
7. B. M. Grafov and E. A. Ukshe, *Electrochemical Circuits of Alternating Current* (Nauka, Moscow, 1973) [in Russian].
8. J. R. Macdonald, *J. Non-Cryst. Solids* **197**, 83 (1996).
9. H. Fröhlich, *Theory of Dielectrics* (Clarendon, Oxford, 1958; Inostrannaya Literatura, Moscow, 1960).
10. F. Alvarez, A. Alegria, and J. Colmenero, *J. Chem. Phys.* **103**, 798 (1995).
11. J. R. Macdonald, *J. Chem. Phys.* **102**, 6241 (1995).
12. H. Schafer, E. Sternin, R. Stannarius, M. Arndt, and F. Kremer, *Phys. Rev. Lett.* **76**, 2177 (1996).
13. B. A. Belyaev, N. A. Drokin, and V. F. Shabanov, *Fiz. Tverd. Tela* (St. Petersburg) **48** (5), 724 (2006) [*Phys. Solid State* **48** (5), 973 (2006)].
14. A. P. Boltaev and F. A. Pudonin, *Zh. Éksp. Teor. Fiz.* **134** (3), 587 (2008) [*JETP* **107** (3), 501 (2008)].

Translated by E. Chernokozhin